Heliyon 10 (2024) e34973

Contents lists available at ScienceDirect

Heliyon

journal homepage: www.cell.com/heliyon

Research article

The TWIK-related acid sensitive potassium 3 (TASK-3) channel contributes to the different effects of anesthetics on the growth and metastasis of ovarian cancer cells

Zhiqiang Hu [a,b,c,1], Qi Jia [a,b,c,1], Shanglong Yao [a,b,c], Xiangdong Chen [a,b,c,*]

[a] Department of Anesthesiology, Union Hospital, Tongji Medical College, Huazhong University of Science and Technology, Wuhan, China
[b] Institute of Anesthesia and Critical Care Medicine, Union Hospital, Tongji Medical College, Huazhong University of Science and Technology, Wuhan, China
[c] Key Laboratory of Anesthesiology and Resuscitation, Huazhong University of Science and Technology, Ministry of Education, Wuhan, 430022, China

ARTICLE INFO

Keywords:
Ovarian cancer
TASK-3 channel
Sevoflurane
Propofol
Lidocaine
Apoptosis

ABSTRACT

Different anesthetics exert different effects on the long-term outcomes of various cancers. The TWIK-related acid sensitive potassium 3 (TASK-3) channel is an important target of anesthetics and is upregulated in various cancers. However, the role and underlying mechanism of TASK-3 channel in the effects of anesthetics on ovarian cancer remain unknown. Here, we tested whether the TASK-3 channel contributes to the effects of anesthetics on ovarian cancers. We found that the TASK-3 channel was overexpressed in human ovarian cancer and ovarian cancer cell lines. Clinically relevant concentrations of lidocaine, as a TASK-3 channel inhibitor, exert inhibitory effects on tumor growth and metastasis of ovarian cancer cells *in vitro* and *in vivo*, whereas the TASK-3 channel potent activator sevoflurane had protumor effects and propofol had no significant effects on tumor growth and metastasis of ovarian cancer. Knockdown of the TASK-3 channel by TASK-3 shRNA attenuated the effects of lidocaine and sevoflurane. Moreover, mitochondrial TASK-3 channel contributes to the effects of lidocaine and sevoflurane on the mitochondrial functions of ovarian cancer. Taken together, the TASK-3 channel, especially the mitochondrial TASK-3 (MitoTASK-3) channel, is a molecular substrate for the effects of lidocaine and sevoflurane on the tumor growth and metastasis of ovarian cancer.

1. Introduction

Ovarian cancer remains the most lethal gynecologic malignancy [1]. Despite significant therapeutic advances, the 5-year survival rate for advanced-stage ovarian cancer remains approximately 30 %, and surgical resection remains the most effective therapeutic strategy for ovarian cancer [1,2]. Growing evidence has indicated that different anesthetic regimens may exert different effects on the postoperative outcome of patients with cancer [3–5]. However, the effects of general and local anesthetics on ovarian cancer remain unclear.

* Corresponding author. Department of Anesthesiology, Union Hospital, Tongji Medical College, Huazhong University of Science and Technology, Wuhan, China.
E-mail address: Xiangdongchenunion@163.com (X. Chen).
[1] Contributed equally.

https://doi.org/10.1016/j.heliyon.2024.e34973
Received 8 February 2024; Received in revised form 17 July 2024; Accepted 19 July 2024
Available online 25 July 2024

Several retrospective studies have consistently demonstrated that volatile anesthetics were associated with higher risks of tumor recurrence and mortality in cancer patients compared with intravenous anesthetics. Volatile anesthetics can inhibit immune cells (e.g., NK cells) [6–8], promote cancer cell proliferation and angiogenesis (via upregulation of hypoxia-inducible factor-1α (HIF-1α)) [9,10], which indirectly and directly accelerates tumor growth and metastasis. Conversely, intravenous anesthetics, especially propofol, were suggested to be beneficial or noninferior for the outcome of patients with cancer (promoting NK cell cytoxicity and downregulation of HIF-1α) [8,11]. Furthermore, compared with general anesthetics, a beneficial role of local anesthetics in attenuating tumor growth and metastasis was suggested [12–14]. Encouragingly, a recent clinical trial reported that peritumoral injection of lidocaine before breast cancer surgery can significantly increases disease-free survival (DFS) and overall survival (OS) [15]. Local anesthetics may exert antitumor effects on cancer cells through indirect (e.g., preservation of immune functions) [8] and direct pathways (e.g., inhibition of cancer cell proliferation through the mitogen-activated protein kinase (MAPK) pathway) [12,16,17]. However, whether there is a shared biological mechanism of anesthetics on ovarian cancer cells requires investigation.

TWIK-related acid sensitive potassium 3 (TASK-3, KCNK9) channel is a member of the two-pore domain potassium channel family [18]. Under physiological conditions, the TASK-3 channel is highly expressed in various tissues, e.g., the central nervous system, serving as a key regulator of cell excitability and hormone secretion [19,20]. The TASK-3 channel underlying currents could be potentiated by volatile anesthetics and inhibited by local anesthetics at clinically relevant concentrations. The TASK-3 channel has been reported to be involved in the sedative, immobilizing and neuroprotective actions of volatile anesthetics and local anesthetic-induced seizures [19,21–23], whereas intravenous anesthetics, such as propofol, have no effects on the TASK-3 channel.

However, dysregulation of the TASK-3 channel has been implicated in cancer biology. TASK-3 channel overexpression at the mRNA and protein levels has been identified in breast, lung and colorectal cancer [24–26], which was suggested to promote malignant transformation and confer resistance to hypoxia and serum deprivation [24]. Inhibition of the TASK-3 channel reduced cell proliferation and induced apoptosis of cancer cells [27], and a monoclonal antibody against the TASK-3 channel significantly attenuated tumor growth and metastasis *in vivo* [28]. Notably, in addition to the plasma membrane, the TASK-3 channel was suggested to be highly expressed in the mitochondrial membrane of cancer cells [29], and the mitochondrial TASK-3 (MitoTASK-3) channel has a crucial role in the regulation of mitochondrial activity. Knockdown of the TASK-3 channel caused mitochondrial depolarization and increased the apoptosis rate of cancer cells [27,30].

In the present study, the effects of anesthetics on ovarian cancer cell proliferation, migration and metastasis were determined *in vitro* and *in vivo*. Furthermore, whether the TASK-3 channel contributes to the effects of anesthetics on ovarian cancer cells was further investigated.

2. Materials and methods

2.1. Bioinformatics

TASK-3 gene expression across cancer types was obtained from The Cancer Genome Atlas project (TCGA, https://tcga-data.nci.nih.gov/tcga/). The TASK-3 gene expression in ovarian cancer data were obtained from the Gene Expression Profiling Interactive Analysis (GEPIA) database (http://gepia.cancer-pku.cn/) which included the TCGA database and Genotype-Tissue Expression (GTEx) database.

Table 1
Detailed information of patients (n = 17).

Characteristics	No. of patients
Ages	
>60	10
≤60	7
Diagnosis	
ovarian cancer	11
non-tumor	6
Histological subtype	
Serous	9
Mucinous	1
Endometrioid	1
Non-tumor	6
FIGO stage	
I-II	5
III -IV	6
Non-tumor	6
Pelvic metastasis	
YES	9
NO	8
Chemotherapy	
YES	0
NO	17

Abbreviation, FIGO, International Federation of Gynecology and Obstetrics.

2.2. Cell cultures and tissue specimens

The human ovarian surface epithelial cell line IOSE-80 and human ovarian cancer cell line SKOV-3 were obtained from ATCC (Manassas, VA, USA). Cells were routinely cultured in RPMI-1640 with 10 % (v/v) fetal bovine serum (FBS) at 37 °C in 5 % CO_2. Ovarian specimens were collected from Union Hospital, Tongji Medical College, Huazhong University of Science and Technology. Patients receiving surgery for suspected serous epithelial ovarian cancer (tumor group), and oophorectomy for other benign gynecological diseases (normal group) were eligible for this study. Clinical and pathological information (age, FIGO stage, pelvic metastasis, etc.) was obtained from clinical records (Table 1). Patients who received platinum-based chemotherapy, which is known to regulate many potassium channels, before surgery were excluded [31].

2.3. Cell proliferation assays

Cell viability was analyzed using the Cell Counting Kit-8 (CCK-8) assay kit (Dojindo Molecular Technologies, Japan). Briefly, SKOV-3 cells were seeded at 5000 cells/well in 96-well plates and subsequently incubated with lidocaine (0.01–5 mM), sevoflurane (1–6%) and propofol (5–100 μM) at the indicated concentrations for 24 h. Thereafter, proliferation was quantified by the addition of CCK-8, plates were incubated for 2–3 h, and the absorbance was then read at 450 nm using a spectrophotometer (Olympus, Japan). Each experiment was repeated three times.

2.4. Cell cycle and apoptosis analysis

Cell cycle phase distribution was monitored by the cellular DNA content, and the DNA content was measured by flow cytometry. The cells were treated in a 6-well plate and incubated for 24 h. Thereafter, SKOV-3 cells were harvested, rinsed twice with PBS and fixed with cold 70 % v/v ethanol at 4 °C. The fixed cells were rinsed twice with PBS and then suspended in 200 μl of Muse Cell Cycle reagent, and incubated at room temperature for 30 min. The populations of SKOV-3 cells in the G_0/G_1, S, and G_2/M phases were calculated using CellQuest Pro software (BD Bioscience, USA).

Cell apoptosis analysis was performed by flow cytometry using the Annexin V-FITC/PI kit (BD Bioscience, USA). After treatment with anesthetics, the cells were harvested and rinsed with PBS, double labelled with fluorescein isothiocyanate conjugated Annexin V-FITC and PI at room temperature for 30 min in the dark, and the apoptosis rate was calculated according to the manufacturer's protocol.

2.5. Transwell cell migration and invasion assays

Cell migration and invasion capacities were detected by Transwell experiments. Cell migration was assayed in a BD chamber (Corning, USA) with transwell polycarbonate filters (8 μm pore size). For the cell invasion assay, the BD chamber was precoated with Matrigel (Corning). Briefly, 5×10^4 SKOV-3 cells were suspended in serum-free RPMI-1640 (200 μl) and placed in the upper chamber. The bottom chamber was filled with 500 μl RPMI-1640 with 10 % FBS. After incubation of 16 h (migration) or 48 h (invasion), cells in the upper chambers were removed by cotton swabs, and cells that had migrated (or invaded through the Matrigel) to the underside of the filter were fixed and stained with crystal violet. Finally, five random regions (200 ×) of the filter were selected to count the number of transmembrane cells. All experiments were repeated three times.

2.6. Mitochondrial labelling and immunofluorescence

Mitochondrial labelling was performed by employing a mitochondrion-selective fluorescent probe (MitoTracker Red, CST). SKOV-3 cells were incubated with MitoTraker Red (200 nM) for 30 min, rinsed with PBS and fixed with 4 % paraformaldehyde, and nonspecific staining was blocked with 3 % bovine serum albumin (BSA)/5 % glycine followed by 10 % goat serum in phosphate-buffered saline (PBS). Cells were then incubated with TASK-3 antibody (1:50) (LifeSpan Bioscience, USA). After washing with PBS three times, cells were incubated with FITC-conjugated secondary antibody (1:50, Antgene, China) for 30 min. Cells were observed under a confocal fluorescence microscope (Nikon, Japan).

2.7. Mitochondrial membrane potential assay

The mitochondrial transmembrane potential (ΔΨm) was analyzed using the ΔΨm-specific dye JC-1 (Invitrogen, USA). In brief, after drug treatment, 5×10^5 cells per sample were rinsed twice with PBS and incubated with 2 μM JC-1 for 20 min. Cells were then rinsed twice, resuspended in PBS, and immediately analyzed in flow cytometer.

2.8. Preparation of mitochondrial and cytoplasmic fractions

The mitochondrial and cytoplasmic fractions were prepared using the Cytosol/Mitochondrial Fractionation kit (Millipoore, USA) according to the manufacturer's instructions. Briefly, 5×10^7 SKOV-3 cells were collected in cold PBS, centrifuged, resuspended in cytosol extraction buffer mix, vortexed, and incubated on ice for 10 min. Samples were centrifuged at 700×*g* for 10 min, and supernatant was transferred and centrifuged at 10000×*g* for 30 min to precipitate mitochondria. The supernatant was stored as the

cytosolic fraction, and the pellet was resuspended in mitochondrial extraction buffer mix as the mitochondrial fraction.

2.9. Quantitative real-time PCR and western blotting

Real-time PCR and Western blot analyses were performed as previously described. For PCR analysis, total RNA was extracted from human specimens and cell lines using TRizol reagent (Life Technologies, USA). The primers used in this study as follows: the human TASK-3 qPCR primers: forward, 5′-ATC ACA CAT CAT AGC CTG CTT TTG-3′; reverse, 5′-CCA TGA CAC ATC AGG GAT AAG AAC T-3′. The human GAPDH qPCR primers: forward, 5′-CCC ATG TTC GTC ATG GGT GT-3′; reverse, 5′-TCG GTC ATG AGT CCT TCC ACG ATA-3′. For western blotting analysis, primary antibodies against TASK-3 channel (Abcam, USA), β-actin (Abcam, USA), cytochrome *c* (CST, USA) and COX IV (Abcam, USA) were used as recommended by the manufacturer.

2.10. Generation of TASK-3 knockdown ovarian cancer cells

Human pLKO.1 lentiviral shRNA target gene against TASK-3 (KCNK9) and pLKO.1-TRC-control vector were synthesized by OBiO Company (Shanghai, China). TASK-3 shRNA mature antisense sequences were as follows: #1: 5′-AAT TCA AAA AGC TTC ATC ACG TTG ACT AC-3′; #2: 5′-AAT TCA AAA ACC ATG AAC AGT GAG GAT GA-3′; and #3: 5′-AAT TCA AAA AGC TGA AGC GCA TTA AGA AG-3′. SKOV-3 cells were transfected with TASK-3 specific and scrambled shRNA vector constructs in antibiotic-free culture medium for 24 h. Polybrene (Millipore) at a final concentration of 10 μg/ml was applied to the medium to enhance virus infection efficiency. Stably transfected colonies were selected in puromycin (10 μg/ml)-containing medium for 4–7 days. Knockdown of the TASK-3 channel was evaluated by RT-PCR and western blotting at different times.

2.11. Xenograft experiments and tail-vein injection in nude mice

Female BALB/c nude mice (16–18 g, 4–6 weeks old) were purchased from Weitonglihua Animal Centre (Beijing, China). The nude mice were randomized to the experimental or control group (n = 6 per group) before beginning the treatment schedule. SKOV-3 cells (2×10^6) or TASK-3 shRNA treated SKOV-3 cells were subcutaneously injected into the right side of the armpits of nude mice. The long (L) and short axes (S) of tumors were measured by calipers, and the tumor volumes (V) were calculated from the formula: $V = (L \times S^2)/2$. When the tumor volume reached approximately 50 mm^3, the mice were injected with a PBS solution as a control, lidocaine (30 mg/kg, i.p., twice a week), sevoflurane (3 %, 4 h, twice a week) and propofol (50 mg/kg, i.p., twice a week). The body weight was also recorded. Tumor growth was observed for 27 days from the first treatment. The maximum tumor volume permitted was 2000 mm^3.

Similarly, in tail-vein injection, SKOV-3 cells (2×10^6) or TASK-3 shRNA treated SKOV-3 cells suspended in 100 μl of PBS were injected intravenously through the tail vein of nude mice. After 27 days of treatment with anesthetics, the mice were sacrificed, and lung metastatic foci were recorded. Then, the lungs of mice were harvested, fixed, sectioned and subjected to H&E staining. Ten pictures were captured from each H&E-stained slide, and total areas of metastatic nodules per field were counted using ImageJ.

2.12. Administration of anesthetics

Sevoflurane was delivered as previously described [10]. Briefly, in the *in vitro* and *in vivo* experiments, SKOV-3 cells or nude mice were exposed to sevoflurane in a 1.5 L airtight gas chamber placed in the incubator at 37 °C, with an in-line sevoflurane-specific vaporizer fed by a supply of a gas mixture containing 21 % O_2 and 5 % CO_2 balanced with N_2. The concentrations of oxygen and sevoflurane in the outlet of the chamber were monitored by anesthetic gas analyzers (Mindray, China). Cells in the control condition for sevoflurane were treated with 21 % O_2 and 5 % CO_2 balanced with N_2. For *in vivo* experiments, nude mice were exposed to sevoflurane plus 60 % O_2 (balanced with N_2).

Furthermore, in *in vitro* experiments, lidocaine was obtained as a hydrochloride salt in the commercially available 20 % solution (Hengrui, China) and diluted into the culture medium at the indicated concentrations (0.01–5 mM). Propofol was purchased from AstraZeneca Company and prepared as a stock solution in dimethyl sulfoxide (DMSO) and diluted into the culture medium at the indicated concentrations (5–100 μM). For *in vivo* experiments, both lidocaine (30 mg/kg) and propofol (50 mg/kg) were injected intraperitoneally twice a week.

2.13. Statistical analysis

Values are expressed as the means ± SEM. Two-way ANOVA was used with treatment condition and time as between-group factors and Bonferroni correction for multiple comparisons. The date for one-group variables were analyzed using one-way ANOVA; post hoc pair comparison used a Bonferroni correction. $p < 0.05$ was considered to be statistically significant.

3. Results

3.1. Effects of anesthetics on the cell growth of ovarian cancer cells in vitro

First, we assessed the *in vitro* effects of a volatile anesthetic (sevoflurane), intravenous anesthetic (propofol) and local anesthetic (lidocaine) on the cell proliferation of SKOV-3 cells. As shown in Fig. 1A, sevoflurane significantly increased SKOV-3 cell viability in a

concentration-dependent manner (EC_{50} was approximately 2.3 ± 1.1 %), and the increment reached a plateau when sevoflurane was ~3 %; therefore, 3 % sevoflurane was used in all subsequent experiments. Conversely, lidocaine inhibited SKOV-3 cell viability in a concentration-dependent manner (EC_{50} was approximately 6.9 ± 0.2 mM); therefore, 5 mM lidocaine was used in all subsequent experiments. Intriguingly, SKOV-3 cell viability was not significantly altered when treated with propofol at clinically relevant concentrations (5–20 μM), but a high concentration of propofol (100 μM) inhibited SKOV-3 cell viability. Next, the effects of anesthetics on the cell cycle status and apoptosis rate of SKOV-3 cells were also examined. As shown in Fig. 1B and C, sevoflurane (3 %) reduced the sub G_0/G_1 population from 62.1 ± 1.4 % (control) to 54.3 ± 2.5 %; correspondingly, compared with control group, the percentage of cells in S phase increased from 27.0 ± 1.0 % (control) to 33.5 ± 2.1 %. The apoptosis rate was reduced by sevoflurane treatment (from 2.3 ± 0.2 % to 1.5 ± 0.1 %). In comparison, after lidocaine (5 mM) treatment, the sub G_0/G_1 population was significantly increased from 62.1 ± 1.4 % (control) to 76.6 ± 2.5 %, and the S phase population decreased from 27.0 ± 1.0 % (control) to 15.9 ± 1.8 %. Meanwhile, lidocaine significantly increased the apoptosis rate of SKOV-3 cells from 2.3 ± 0.2 % (control) to 10.9 ± 0.9 %. However, propofol (20 μM) had no effects on cell cycle or apoptosis rate of SKOV-3 cells.

3.2. *Effects of anesthetics on cell migration and invasion of ovarian cancer cells in vitro*

Next, the *in vitro* effects of anesthetics on SKOV-3 cell migration and invasion were investigated. As illustrated in Fig. 2A and B, compared with the control group, the number of migrating cells in the sevoflurane group (3 %) was significantly increased (from 83.8 ± 2.8 to 115.2 ± 5.9), and sevoflurane also markedly increased the number of invading cells (from 63.8 ± 3.7 to 81.8 ± 3.5). The EC_{50} values of the increment of sevoflurane on SKOV-3 cancer cell migration and invasion were approximately 2.8 ± 1.2 % and 2.5 ± 1.0 %, respectively, whereas treatment with propofol (20 μM) significantly reduced the number of migrating and invading cells (from 83.8 ± 2.8 to 73.0 ± 3.1 and from 63.8 ± 3.7 to 51.8 ± 3.0, respectively). The EC_{50} values of inhibition of propofol on cancer cell migration and invasion were approximately 21.5 ± 1.2 μM and 20.6 ± 1.2 μM, respectively. Additionally, lidocaine (5 mM) treatment also significantly reduced the number of migrating and invading cells (from 83.8 ± 2.8 to 25.4 ± 3.6 and from 63.8 ± 3.7 to 15.3 ± 2.3, respectively), and the EC_{50} values of inhibition of lidocaine on cancer cell migration and invasion were approximately 1.7 ± 0.2 mM

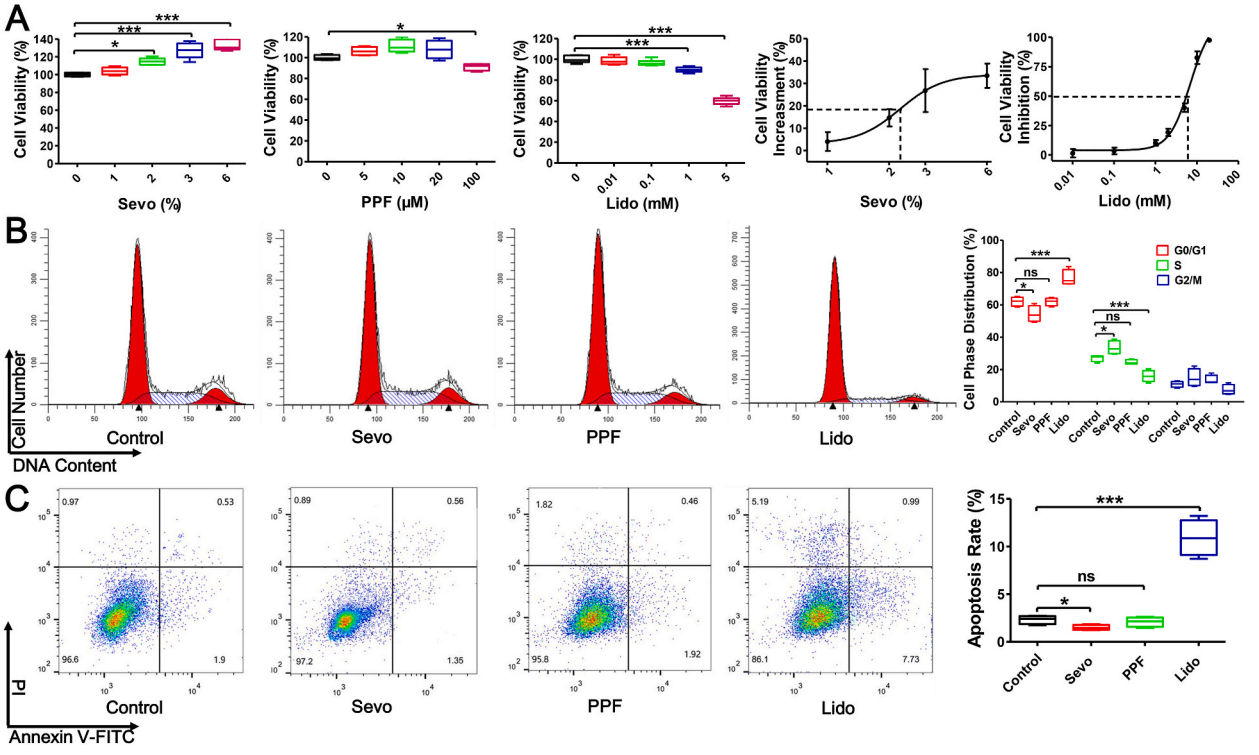

Fig. 1. Effects of anesthetics on the cell growth and apoptosis of ovarian cancer cells (A) Effects of anesthetics on the cell viability of SKOV-3 cells. Treatment with sevoflurane (Sevo, n = 5) significantly increased the cell viability of SKOV-3 cells in a concentration-dependent manner (EC50 was 2.3 ± 1.1 %); clinically relevant concentrations of propofol (PPF, 5–20 μM, n = 4) had no effect on the cell viability of SKOV-3 cells, whereas a higher concentration of propofol (100 μM) inhibited the cell viability; lidocaine (Lido, n = 6) resulted in significant reductions in cell viability in a concentration-dependent manner (EC50 was 6.9 ± 0.2 mM). Statistical differences were determined using a one-way ANOVA. (**B–C**) Representative image showing the effects of anesthetics on cell cycle progression and apoptosis rate of SKOV-3 cells. Treatment with sevoflurane (3 %, n = 4, *t*-test) significantly increased the percentage of G0/G1 phase **(B)** and decreased the apoptosis rate of SKOV-3 cells **(C)**; lidocaine (5 mM, n = 4, *t*-test) caused G0/G1 phase arrested **(B)** and increased the apoptosis rate **(C)**, whereas propofol (20 μM, n = 4,*t*-test) had no effects **(B–C)**. These results are expressed as the mean ± SEM, *P < 0.05, *P < 0.01, ***P < 0.001, ns, no significance. FITC = fluorescence isothiocyanate.

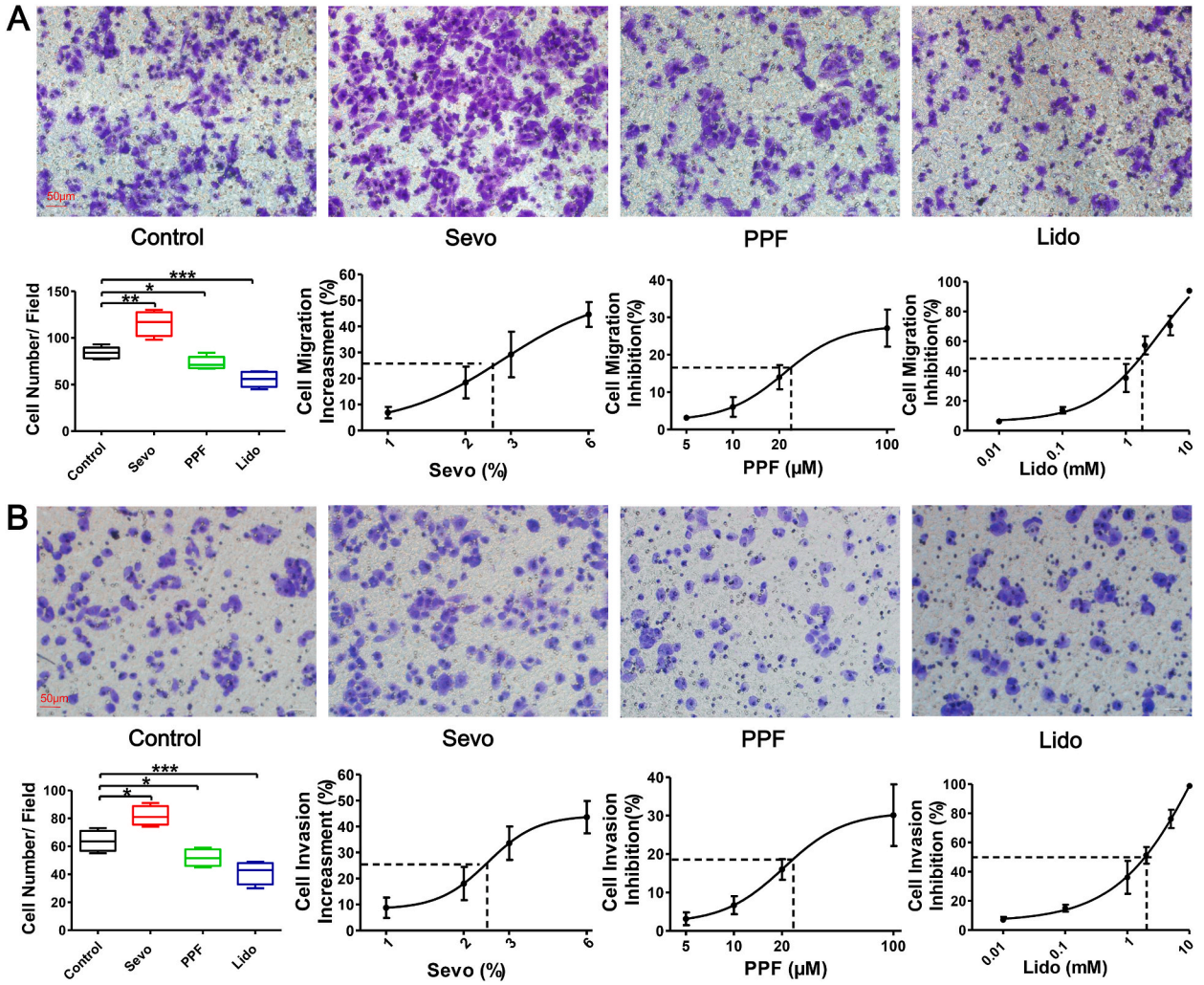

Fig. 2. Effects of anesthetics on cell migration and invasion of ovarian cancer cells (**A-B**) Effects of anesthetics on cell migration and invasion of SKOV-3 cells. Sevoflurane (Sevo, 3 %) significantly promoted the cell migration and invasion of SKOV-3 cells (EC50 was 2.8 ± 1.2 % and 2.5 ± 1.0 %, respectively, **A-B**); propofol (PPF, 20 μM) caused slight but significant inhibition of cell migration and invasion (EC50 was 21.5 ± 1.2 μM and 20.6 ± 1.2 μM, respectively, **A-B**); but lidocaine (Lido, 5 mM) significantly inhibited the cell migration and invasion of SKOV-3 cells (EC50 was 1.7 ± 0.2 mM and 1.8 ± 0.3 mM, respectively, **A-B**). These results are expressed as the mean ± SEM. Statistical differences were determined using unpaired *t*-test or one-way ANOVA. *P < 0.05, *P < 0.01, ***P < 0.001, n = 5 in each group. Scale bar, 50 μm.

and 1.8 ± 0.3 mM, respectively, suggesting that SKOV-3 cell migration and invasion were more susceptible to inhibition than cell growth after lidocaine treatment.

3.3. *Effects of anesthetics on tumor growth and lung metastasis of ovarian cancer cells in vivo*

Then, the *in vivo* effects of anesthetics on tumor growth and lung metastasis of SKOV-3 cell xenografts were examined. As shown in Fig. 3A and B, compared with the control group, the tumor volume and weight were significantly greater in sevoflurane group (3 %, 4 h, twice a week); and lidocaine treatment (30 mg/kg, i.p., twice a week) significantly suppressed tumor growth and tumor weight; propofol treatment (50 mg/kg, i.p., twice a week) failed to exert inhibitory effects on tumor growth. Similarly, as shown in Fig. 3C and D, compared with control group, sevoflurane significantly increased the number of lung metastases (24.2 ± 2.1 vs. 13.0 ± 1.6), but lidocaine-treated nude mice showed significantly fewer lung metastases compared with the control group (5.3 ± 1.1 vs. 13.0 ± 1.6). Propofol had no significant effects on lung metastases of ovarian cancer.

3.4. *TASK-3 channel is overexpressed in human ovarian cancer*

Accumulating evidence indicates that the TASK-3 channel is upregulated in several cancers [24–26,30]. As illustrated in Fig. 4A,

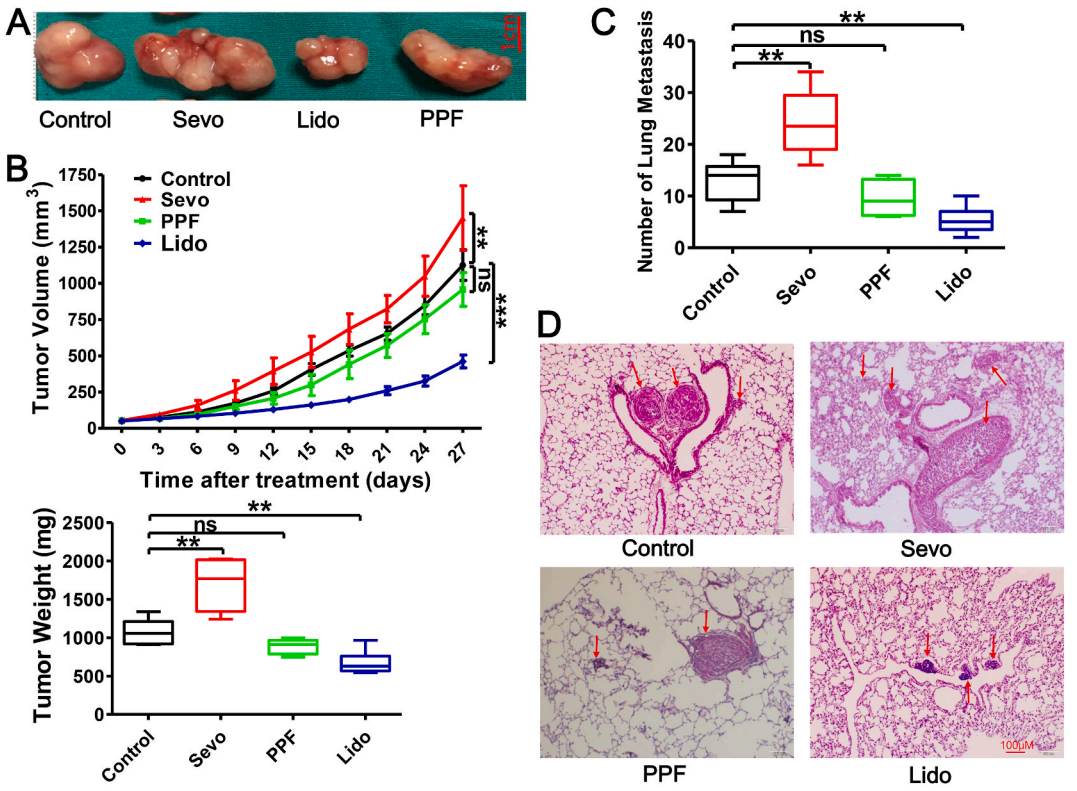

Fig. 3. Effects of anesthetics on tumor growth and lung metastasis of SKOV-3 cells xenografts in nude mice **(A)** Representative sample of the dissected ovarian tumor tissues treated with anesthetics (sevoflurane, propofol and lidocaine), scale bar, 1 cm. **(B)** Growth curves and tumor weight of SKOV-3 engraftments in nude mice treated with anesthetics twice a week for 27 days. Sevoflurane (3 %) significantly promoted the tumor growth and increased the tumor weight of SKOV-3 engraftments; lidocaine (Lido, i.p., 30 mg/kg) significantly inhibited the tumor growth and decreased the tumor weight; whereas propofol (PPF, i.p., 50 mg/kg) had no effects. **(C–D)** Numbers and representative images of lung metastatic foci in nude mice treated with anesthetics twice a week for 27 days. Sevoflurane (3 %) significantly promoted but lidocaine (30 mg/kg) significantly inhibited the lung metastasis (red arrows) of SKOV-3 engraftments, whereas propofol (50 mg/kg) had no effects, scale bar, 100 μM. These results are expressed as the mean ± SEM. Statistical differences were determined using a two-way ANOVA or unpaired *t*-test. *P < 0.05, *P < 0.01, ***P < 0.001, ns, no significance, n = 5 in each group.

the expression of the TASK-3 channel in cancers based on high-throughput RNA-sequencing data from the TCGA database showed a significant upregulation in 14 TCGA cancer types and high expression in ovarian cancer. Next, we mined TASK-3 channel expression in ovarian cancer from the GEPIA database and found that TASK-3 channel expression in ovarian cancer (n = 426) was significantly higher than that in normal ovarian tissues (n = 88, Fig. 4B).

Then, we tested the bioinformatics results in human ovarian specimens and ovarian cancer cell lines. As shown in Fig. 4C and D, the protein level of the TASK-3 channel in human ovarian cancer (0.80 ± 0.12) was approximately 2-fold higher than that in human normal ovaries (0.42 ± 0.04). Similarly, compared with human ovarian surfaced epithelial line IOSE-80, there were significant increases in TASK-3 channel expression in the human ovarian cancer cell line SKOV-3 (mRNA: increased ~2.6 fold; protein: increased ~0.97 fold).

3.5. TASK-3 knockdown attenuated the effects of sevoflurane and lidocaine on the apoptosis rate, cell migration and invasion of SKOV-3 cells

Next, SKOV-3 cells were stably transfected with a specific shRNA sequence. As shown in Fig. 5A and B, the cell line denoted as shRNA1 showed the greatest reduction in mRNA and protein levels of the TASK-3 channel, without influencing the expression of other K2P channels (TASK-1, TREK-1/2 and TRAAK). However, cell lines that had been transfected with a scramble shRNA sequence did not present appreciable changes in TASK-3 channel expression. Given that the shRNA1 construct showed greater specificity for the TASK-3 channel, this construct was chosen for the next set of experiments.

Furthermore, we investigated the proliferative effects of TASK-3 channel knockdown in SKOV-3 cells. As shown in Fig. 5C, there was a significant reduction in the cell viability of shRNA1-treated cells compared with the control group (84.7 ± 2.4 % vs. 100.0 ± 1.8 %). Given that the TASK-3 channel has also been implicated in the anesthetic actions of local and volatile anesthetics, we examined whether the TASK-3 channel contributes to the effects of lidocaine and sevoflurane on ovarian cancer. In Fig. 5D, the apoptosis rate was

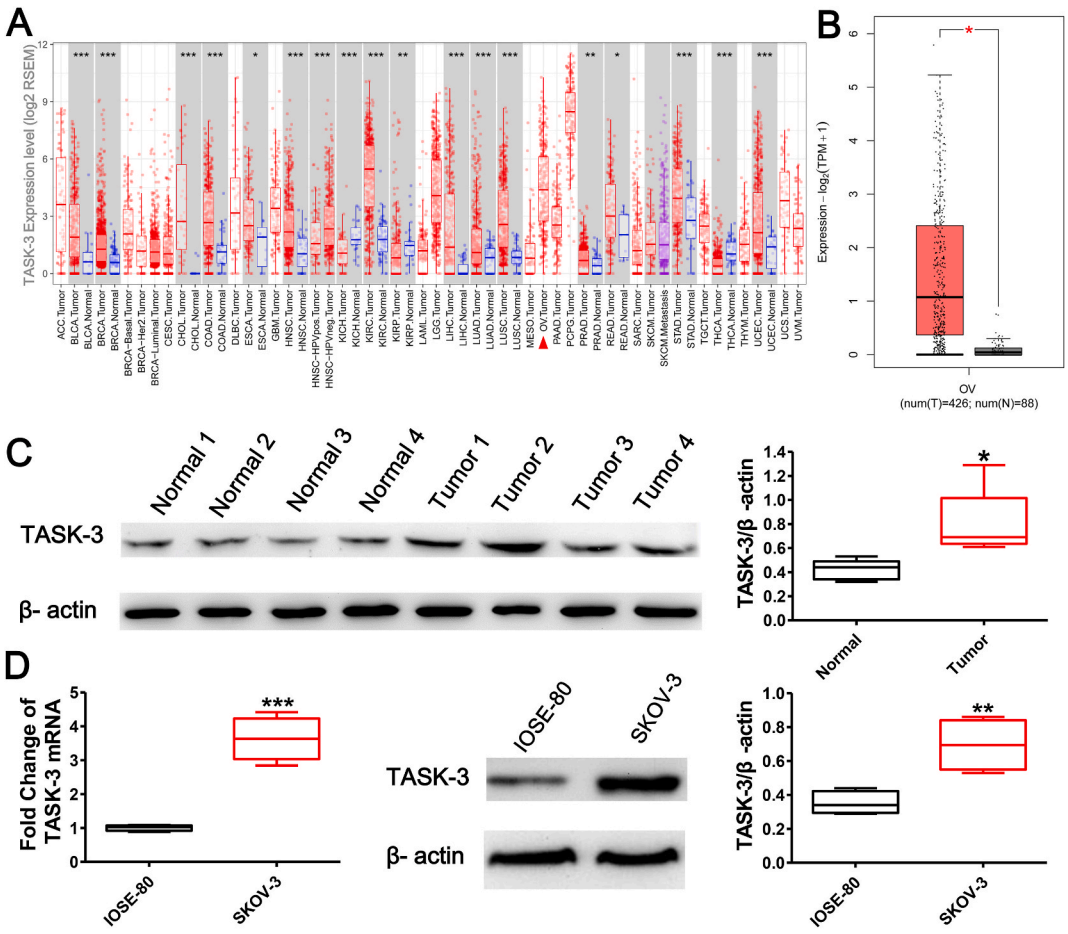

Fig. 4. TASK-3 channel is overexpressed in ovarian cancer **(A)** Bioinformatics analysis of TASK-3 channel expression in various cancers from the TCGA database, red triangle indicates the ovarian cancer, OV = ovarian cancer. **(B)** Bioinformatics analysis of TASK-3 channel expression in ovarian cancer form the Gepia database. **(C)** Representative western blotting and quantitative analysis of the protein levels of TASK-3 channel in human ovarian cancer and normal ovaries. TASK-3 channel is overexpressed in human ovarian cancer compared with normal ovaries (n = 5). **(D)** Relative expression of TASK-3 mRNA and protein in human normal ovarian epithelial cell line IOSE-80 and ovarian cancer cell line SKOV-3. The mRNA and protein levels of TASK-3 channel were upregulated in SKOV-3 compared with IOSE-80 (n = 5). These results are expressed as the mean ± SEM. Statistical differences were determined using unpaired *t*-test, *P < 0.05, *P < 0.01, ***P < 0.001.

2.3 ± 0.2 % in the control group, and sevoflurane (3 %) significantly reduced the apoptosis rate (1.5 ± 0.1 %), but lidocaine (5 mM) markedly increased the apoptosis rate of SKOV-3 cells (10.9 ± 0.9 %). Moreover, the apoptosis rate was significantly increased in the TASK-3 shRNA group (4.0 ± 0.3 %). Compared with the sevoflurane group, TASK-3 channel knockdown attenuated the effects of sevoflurane (3.3 ± 0.2 % vs.1.5 ± 0.1 %). Lidocaine failed to evoke significant changes in the apoptosis rate in TASK-3 shRNA-treated cells, and pretreatment with TASK-3 shRNA attenuated but failed to abolish the proapoptotic effects of lidocaine (7.1 ± 0.6 % vs. 10.9 ± 0.9 %), indicating that other mechanisms may also contribute to the effects of lidocaine.

Likewise, as shown in Fig. 6A and B, compared with control group, sevoflurane significantly increased the numbers of migrating and invading SKOV-3 cells, but lidocaine exerted the opposite effects, which markedly reduced the numbers of migrating and invading cancer cells. There were no significant changes in cell migration and invasion between the TASK-3 shRNA and TASK-3 shRNA plus lidocaine groups. Pretreatment with TASK-3 shRNA attenuated the effects of lidocaine and sevoflurane.

3.6. *TASK-3 knockdown abated the effects of sevoflurane and lidocaine on tumor growth and lung metastasis of ovarian cancer cells in vivo*

Additionally, the functional roles of TASK-3 channels in the *in vivo* effects of anesthetics on tumor growth and lung metastasis of ovarian cancer were examined. In Fig. 7A–C, TASK-3 channels knockdown resulted in a slower growth rate compared with the control group, the tumor volume was significantly smaller (734.2 ± 33.1 mm^3 vs. 1125.5 ± 46.9 mm^3) and the tumor weight was also significantly decreased (753.0 ± 44.5 mg vs. 1075.4 ± 67.8 mg) after 27 days. Meanwhile, TASK-3 shRNA-treated mice showed significantly fewer lung metastases than the control group (9.0 ± 0.7 vs. 13.0 ± 1.6). Moreover, compared with the lidocaine group, lidocaine treatment failed to evoke any significant changes in tumor growth, tumor weight and lung metastases in TASK-3 shRNA-

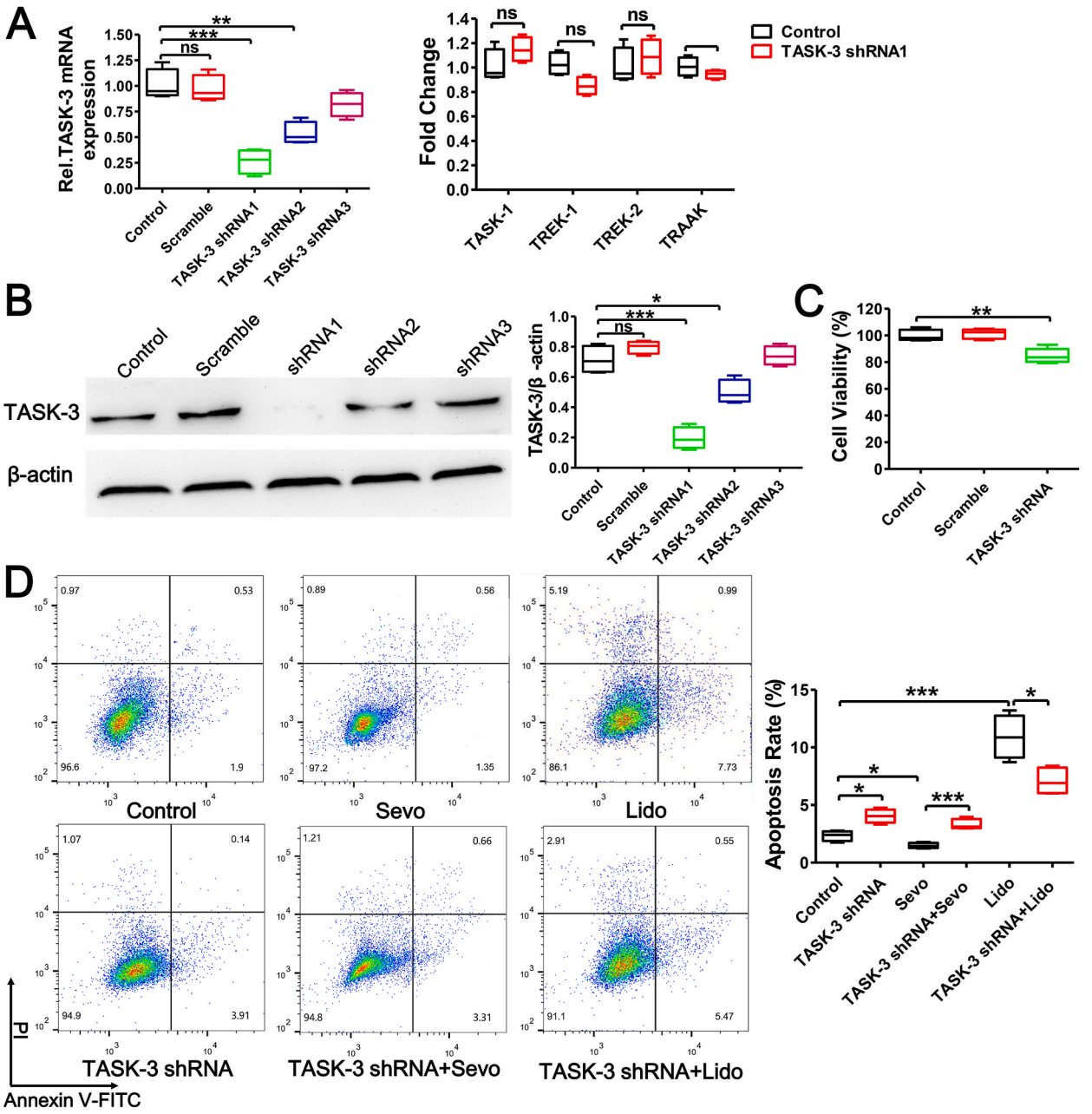

Fig. 5. TASK-3 shRNA attenuated the effects of lidocaine and sevoflurane on cell growth and apoptosis rate of SKOV-3 cells. (A-**B)** Relative expression of TASK-3 mRNA and protein in SKOV-3 cells treated with TASK-3 shRNA, scramble shRNA or control group. **(A–B)** The cell line denoted as shRNA1 shown the greatest reduction of mRNA and protein levels of TASK-3 channel but no effects on other K2P channels. **(C)** TASK-3 shRNA treatment significantly reduced the cell viability of SKOV-3 cells. **(D)** Sevoflurane (Sevo, 3 %) significantly decreased the apoptosis rate of SKOV-3 cells, but lidocaine (Lido, 5 mM) and TASK-3 shRNA significantly increased the apoptosis rate, and pretreatment with TASK-3 shRNA attenuated the effects of sevoflurane and lidocaine on apoptosis rate of SKOV-3 cells. These results are expressed as the mean ± SEM. Statistical differences were determined using unpaired *t*-test, *P < 0.05, *P < 0.01, ***P < 0.001, ns, no significance, n = 4 in each group.

treated mice, and TASK-3 channel knockdown attenuated the effects of sevoflurane on tumor growth, tumor weight and lung metastases of ovarian cancer.

3.7. The TASK-3 channel is highly expressed in the mitochondria of ovarian cancer cells

Furthermore, the mitochondrial TASK-3 (MitoTASK-3) channel, has been reported to play a crucial role in the regulation of

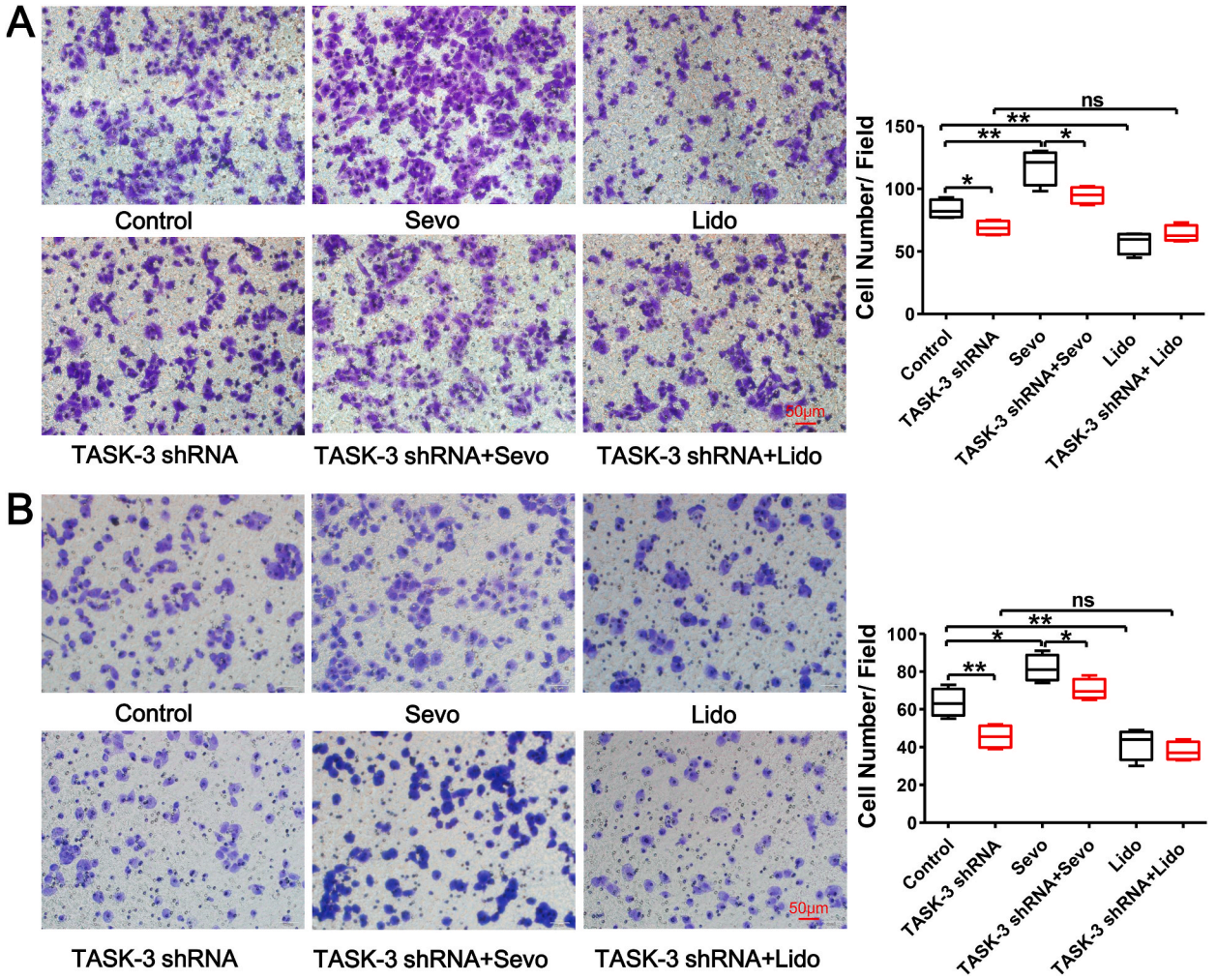

Fig. 6. TASK-3 shRNA attenuated the effects of sevoflurane and lidocaine on cell migration and invasion of SKOV-3 cells. (A-**B)** Changes of the cell migration and invasion of SKOV-3 cells treated with lidocaine, sevoflurane in the absence or presence of TASK-3 shRNA. Sevoflurane (Sevo, 3 %) significantly promoted the cell migration **(A)** and invasion **(B)** of SKOV-3 cells, but lidocaine (Lido, 5 mM) and TASK-3 shRNA significantly inhibited cell migration **(A)** and invasion **(B)** of SKOV-3 cells, but pretreatment of TASK-3 shRNA attenuated the effects of sevoflurane and lidocaine on cell migration and invasion of SKOV-3 cells. These results are expressed as the mean ± SEM. Statistical differences were determined using unpaired *t*-test, *P < 0.05, *P < 0.01, ***P < 0.001, ns, no significance. n = 4 in each group. Scale bar, 50 μm.

mitochondrial activity in cancer cells [26,29]. As illustrated in Fig. 8A, in addition to the plasma membrane and nuclei, TASK-3 channel was highly expressed in the mitochondria of SKOV-3 cells. The distribution of the mitochondrion-specific labeler (Mito-Tracker Red) was almost perfectly identical to that of TASK-3 specific immunopositivity. Furthermore, in the western blotting experiment, TASK-3 specific labelling was observed in the membrane fractions that contained the mitochondrial membrane (as indicated by the presence of the mitochondrial enzyme COX IV), further confirming that the TASK-3 channel is highly expressed in the mitochondrial membrane of ovarian cancer (Fig. 8B).

3.8. TASK-3 knockdown attenuated the effects of sevoflurane and lidocaine on the mitochondrial function of ovarian cancer cells

The roles of TASK-3 channels in the effects of lidocaine and sevoflurane on the mitochondrial function of ovarian cancer cells were then examined. Mitochondrial membrane potential (ΔΨm) is a key index that reflects mitochondrial function. Mitochondrial function was monitored by applying JC-1. A drop in ΔΨm, which is one of the earliest events in apoptosis, results in an increase in JC-1 monomers. As shown in Fig. 8C, compared with control group, sevoflurane (3 %) significantly decreased the percentage of JC-1 monomers (from 3.9 ± 0.3 % to 3.0 ± 0.2 %), but lidocaine (5 mM) markedly increased the percentage of JC-1 monomers (from 3.9 ± 0.2 % to 16.2 ± 0.8 %). The percentage of JC-1 monomers was also significantly increased by knockdown of the TASK-3 channel using TASK-3 shRNA (from 3.9 ± 0.2 % to 8.1 ± 0.4 %). Furthermore, knockdown of the TASK-3 channel attenuated the effects of sevoflurane and lidocaine on the mitochondrial membrane potential in ovarian cancer.

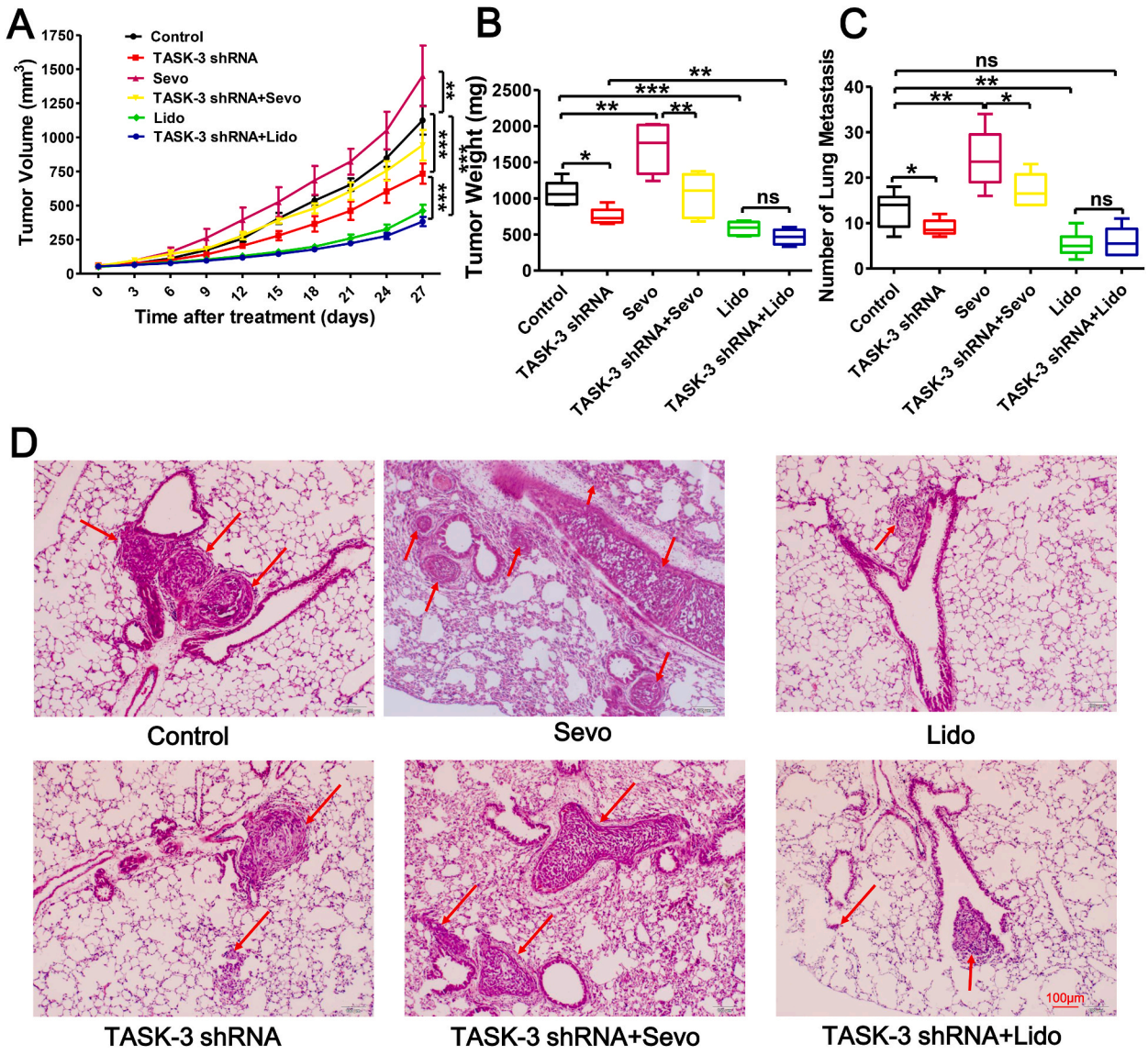

Fig. 7. TASK-3 shRNA attenuated the effects of lidocaine and sevoflurane on tumor growth and lung metastasis of SKOV-3 cells xenografts in nude mice. (A–**B)** Growth curves and tumor weight of SKOV-3 engraftments in nude mice treated with anesthetics (sevoflurane, propofol and lidocaine) in the presence or absence TASK-3 shRNA. **(C–D)** Numbers and representative images of lung metastatic foci in nude mice treated with anesthetics in the presence or absence TASK-3 shRNA. Lidocaine (Lido, i.p., 30 mg/kg) significantly inhibited but sevoflurane (3 %) promoted the lung metastasis (red arrows) of SKOV-3 engraftments. Pretreatment of TASK-3 shRNA attenuated the effects of lidocaine and sevoflurane on the lung metastasis of SKOV-3 engraftments. These results are expressed as the mean ± SEM. Statistical differences were determined using unpaired *t*-test or two-way ANOVA with Bonferroni post hoc *t*-test. *P < 0.05, *P < 0.01, ***P < 0.001, ns, no significance, n = 5 in each group. Scale bar, 100 μm.

Similarly, cytochrome *c* is released from mitochondria into the cytosol, which is also a crucial early event of apoptosis. As shown in Fig. 8D, lidocaine induced the pro-apoptotic release of cytochrome *c*, which was strongly pronounced after treatment with lidocaine at 5 mM (but not 1 mM, data not shown). Compared with the control group, the expression of cytochrome *c* in the cytosol was significantly increased in the lidocaine group. Conversely, the expression of cytochrome *c* in mitochondria was decreased. TASK-3 shRNA treatment of cells also promoted the release of cytochrome *c*, and knockdown of the TASK-3 channel attenuated the effect of lidocaine on the release of cytochrome *c* from ovarian cancer cells.

4. Discussion

In this study, our main findings revealed that the TASK-3 channel is overexpressed in ovarian cancer. The TASK-3 channel inhibitor lidocaine exerts inhibitory effects on tumor growth and metastasis of ovarian cancer cells *in vitro* and *in vivo*, whereas the TASK-3

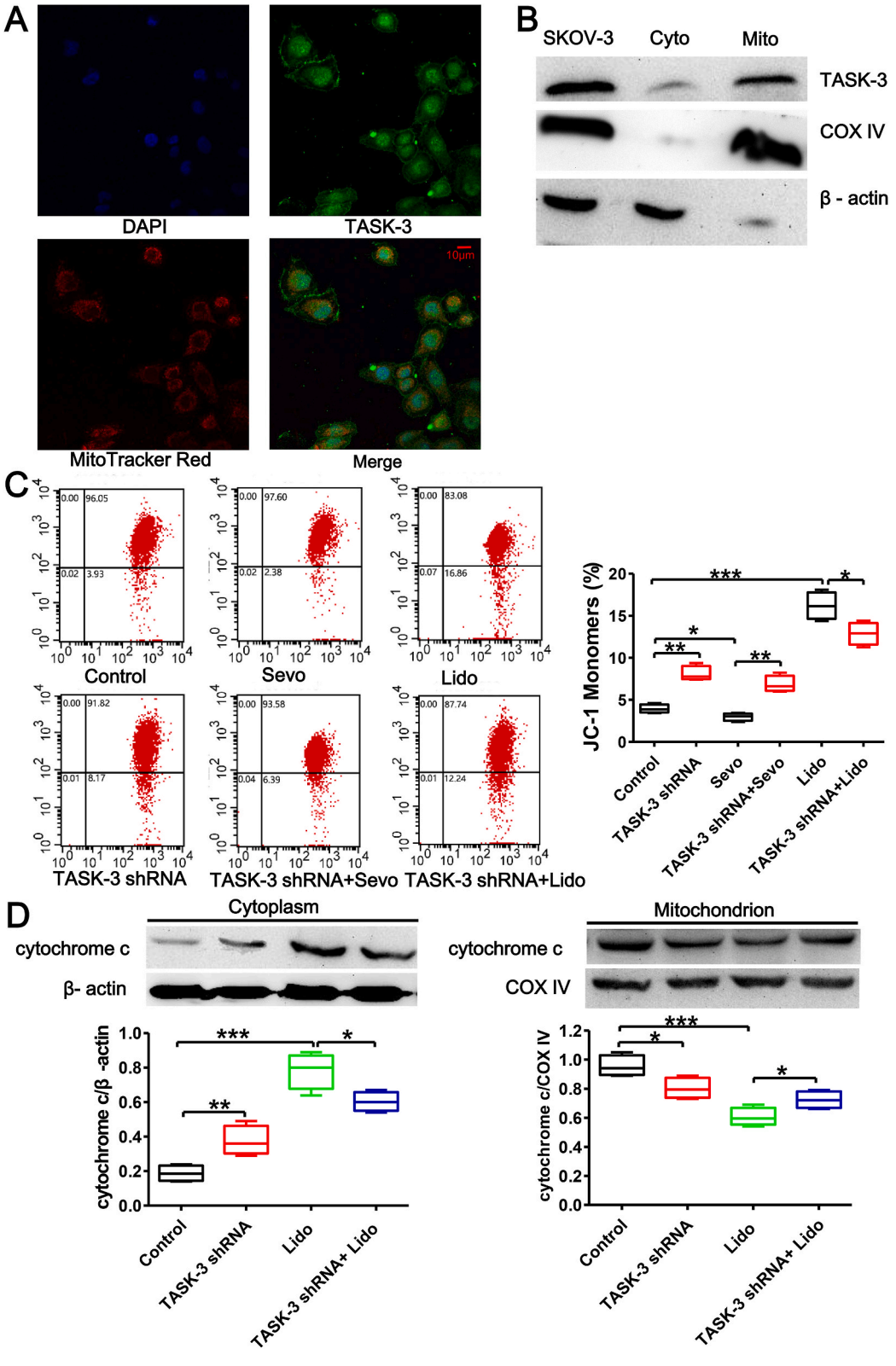

(caption on next page)

Fig. 8. TASK-3 shRNA attenuated the effects of lidocaine and sevoflurane on mitochondrial membrane potential and cytochrome *c* release of SKOV-3 cells (**A)** Expression pattern of TASK-3 channels in SKOV-3 cells. MitoTracker Red: mitochondrion-specific label. TASK-3 channels were highly expressed in the mitochondria of SKOV-3 cells. Scale bar, 10 μm. **(B)** Quantitative analysis of TASK-3 channel expression of total cell lysates, cytoplasm (Cyto) and mitochondrial membrane (Mito) fraction. COX IV, mitochondrial marker. **(C)** Effects of anesthetics on the mitochondrial membrane potential of SKOV-3 cells were determined by JC-1 assay. Lidocaine (Lido, 5 mM) and TASK-3 shRNA caused mitochondrial membrane potential depolarized. Sevoflurane (Sevo, 3 %) significantly hyperpolarized mitochondrial membrane potential, pretreatment of TASK-3 shRNA attenuated the effects of lidocaine and sevoflurane on mitochondrial membrane potential. **(D)** Expressions of cytochrome *c* of cytoplasm and mitochondrial membrane fraction treated with lidocaine (5 mM) in the absence or presence of TASK-3 shRNA. Lidocaine and TASK-3 shRNA caused cytochrome *c* released from mitochondrion to cytoplasm, and TASK-3 shRNA attenuated the effect of lidocaine on cytochrome *c* release. These results are expressed as the mean ± SEM. Statistical differences were determined using unpaired *t*-test. *P < 0.05, *P < 0.01, ***P < 0.001, n = 4 in each group.

channel potent activator sevoflurane had protumor effects and propofol had no significant effects on tumor growth and metastasis of ovarian cancer. Knockdown of the TASK-3 channel by transfection with TASK-3 shRNA attenuated the effects of lidocaine and sevoflurane. Moreover, mitochondrial TASK-3 (MitoTASK-3) channel may contribute to the effects of lidocaine and sevoflurane on the mitochondrial functions of ovarian cancer. In conclusion, the TASK-3 channel, especially the mitochondrial TASK-3 (MitoTASK-3) channel, is a molecular substrate for the effects of lidocaine and sevoflurane on the tumor growth and metastasis of ovarian cancer.

Emerging data indicate that local anesthetics may exert beneficial action in improving the long term outcomes of cancers [8,12,32]. In our study, lidocaine significantly inhibited ovarian cancer cell viability, migration and invasion *in vitro* and suppressed tumor growth and metastasis *in vivo*, which was consistent with the antitumor effects of lidocaine observed on breast, lung and hepatic cancers [12,16,17,33]. Notably, lidocaine at lower concentrations (0.1 mM) also inhibited the migration and invasion of SKOV-3 cells but had no effect on cell viability, suggesting that cancer cell migration and invasion were more susceptible to inhibition than cell growth after lidocaine treatment. Moreover, in our study, lidocaine (5 mM) significantly increased the G0/G1 population and decreased the percentage of cells in S phage, without affecting the G2/M phase. Lidocaine was previously reported to reduce G1/S transition by upregulating cyclin dependent kinase inhibitor 1A and 1b (Cdkn 1a and Cdkn 1b) and downregulating cyclin-dependent kinase 2 (CDK2) and cyclin A expression [34,35], and previous study also indicated that TASK-3 knockdown induces breast cancer cell cycle arrest by upregulating Cdkn 1a and Cdkn 1b [36]. Thus, it is possible that lidocaine suppress the G1/S transition of ovarian cancer cells by downregulating cell-cycle-related proteins (e.g., inhibiting CDK2 and cyclin A expression) and upregulating Cdkn 1a and Cdkn 1b. Furthermore, the intraperitoneal administration of lidocaine (30 mg/kg) was previously reported to inhibit the tumor growth of hepatocellular carcinoma and enhance sensitivity to cisplatin treatment [12]. Likewise, in our study, lidocaine (30 mg/kg) treatment not only suppressed xenografted ovarian cancer growth but also reduced lung metastasis *in vivo*.

Our data also showed that sevoflurane significantly enhance ovarian cancer cell growth and metastasis *in vitro* and *in vivo*, which was consistent with previous findings that volatile anesthetics directly enhanced the malignant potential of breast, renal and ovarian cancer and glioblastoma [9,10,37–39]. However, other studies have shown that volatile anesthetics exert antitumor effects on several cancer cell lines, e.g., the non-small cell lung cancer cell line-A549 [40]. Intriguingly, very low expression of the TASK-3 channel in A549 cells was found in a previous study [41]. Thus, whether the differential effects of volatile anesthetics on different types of cancers are attributed to the expression of TASK-3 channels warrants further investigation. Moreover, compared with volatile anesthetics, the beneficial antitumor effects of propofol have been reported in several studies [3,8,11]. In this study, propofol, at clinically relevant concentrations, inhibited the migration and invasion capabilities of ovarian cancer, but had no effect on cancer growth *in vitro* and *in vivo* or lung metastasis *in vivo*, and the detailed underlying mechanisms need further investigation. In summary, our results indicated that sevoflurane had protumor effects but lidocaine had antitumor effects on the tumor growth and metastasis of ovarian cancer, and further prospective randomized clinical trials comparing the effects of anesthetics on ovarian cancer outcomes might yield more definitive data.

Furthermore, upregulation of the TASK-3 channel in ovarian cancer cells was also identified in our study, which consistent with previous findings that the TASK-3 channel is overexpressed in numerous cancers [24,25,28], and we further confirmed that TASK-3 channels knockdown inhibited ovarian cancer cell growth, attenuated the ability of migration and invasion *in vitro* and slowed tumor growth with fewer lung metastatic foci *in vivo*. In other words, TASK-3 channels confer the malignant potential of ovarian cancer. Local anesthetics at clinically relevant concentrations can significantly inhibit TASK-3 channels underlying currents by interacting with the second pore helices of TASK-3 channel [23,42], exhibiting antigrowth and antimetastatic activity on ovarian cancer similar to the results of knockdown of the TASK-3 channel. However, sevoflurane can strongly activate TASK-3 channels by interacting with the residue M159 at the cytoplasmic terminus of the M3 segment and residues 243 to 248 at the beginning of the cytoplasmic C-terminus of TASK-3 channel [43]. In our study, sevoflurane promotes tumor growth and metastasis *in vitro* and *in vivo*. TASK-3 channel knockdown attenuated the antitumor effects of lidocaine and the protumor effects of sevoflurane on ovarian cancer *in vitro* and *in vivo*, indicating that the TASK-3 channel mediates the differential effects of anesthetics on ovarian cancer. Since these anesthetics are non-sepecific drugs targeting TASK-3 channel, besides the direct effects of these anesthetics on TASK-3 channel, whether these anesthetics indirectly affect TASK-3 channels in ovarian cancer by regulating other pathways or proteins (e.g., ERK1/2) requires further investigation [44,45]. In addition, TASK-3 channel knockdown failed to abolish the effects of lidocaine and sevoflurane on ovarian cancer, suggesting that other molecular mechanisms may also contribute to the antitumor effects of lidocaine and the protumor effects of sevoflurane. Moreover, there are no differences in tumor growth and metastasis in lidocaine and lidocaine plus TASK-3 shRNA groups, it may be caused by several factors (e.g., small sample size, dose and frequency of drug administration, and cancer complexity).

Numerous studies have suggested that cancer cells have more hyperpolarized mitochondrial membrane potential (ΔΨm) than

noncancerous cell lines [46,47], which confers malignant potential (e.g., resistance to apoptosis) to cancer cells. In keeping with this, our studies also found that the ΔΨm of SKOV-3 cells was hyperpolarized by sevoflurane treatment and associated with a decreased apoptosis rate, whereas lidocaine exerted the opposite effects on the ΔΨm and apoptosis rate. Furthermore, TASK-3 channels were highly expressed in the mitochondria of ovarian cancer cells, which was like that found in melanoma. Mitochondrial dysfunction, e.g., depolarization of ΔΨm, has been suggested to participate in the induction of apoptosis and subsequently activate the apoptotic cascade, including the release of cytochrome *c* [48]. Intriguingly, inhibition of MitoTASK-3 channels by lidocaine treatment triggered activation of the apoptotic machinery (e.g., release of cytochrome *c*). Conversely, activation of MitoTASK-3 channels by sevoflurane inhibited the activation of the apoptotic machinery. Moreover, activation of TASK-3 channel expressed in the plasma membrane induces plasma membrane hyperpolarization, which may subsequently increases Ca^{2+} influx and activates several signaling pathways that promote tumor growth and metastasis [28]. Thus, the TASK-3 channel in the plasma membrane may also contribute to the effects of lidocaine and sevoflurane on ovarian cancer cells. Furthermore, in addition to the plasma membrane and mitochondria, the TASK-3 channel was highly expressed in the ovarian cancer cell nucleus, like nuclear Kv1.3, which may contribute to regulating nuclear membrane potential and activating transcription factors, such as phosphorylated CREB and c-fos [49].

Our finding may have several important clinical implications: administration of local anesthetics may be an easy, cost-effective therapeutic intervention; the circulating concentration of lidocaine in *in vivo* experiments is relevantly low, and periopeartive infiltration of local anesthetics around the tumor may be a more promising antitumor intervention that prolong overall survival in patients, as well as reducing intraoperative volatile anesthetics use may offer a clinically meaningful improvement of oncological outcomes. However, there are still several limitations in our study. First, since NK cell activity could be influenced by anesthetics, nude mice were used in our study, which were T-cell deficient but had enhanced NK cell activity, thus, some severely immunodeficient mice (e.g., NOD/Scid mice) are better at determining the effects of anesthetics on ovarian cancer [50]. Second, in our study, we established cell line-derived xenografts in nude mice as a preclinical model, but patient-derived xenografts are believed to conserve original tumor characteristics (e.g., heterogeneous histology, malignant genotypes, tumor architecture and tumor vasculature) [51] and may be more valuable for evaluating the effects of anesthetics on the clinical outcomes of ovarian cancer. Third, owing to the smaller size and intricate morphology of mitochondria, especially the inner mitochondrial membrane, we failed to record the MitoTASK-3 channel underlying currents in ovarian cancer cells, and further studies are needed to examined the electrophysiological effects of anesthetics on the MitoTASK-3 channel. In addition, according to the data obtained from TCGA database (Fig. 4A), we found that TASK-3 is overexpressed in various types of cancers, whether TASK-3 channels also contribute to the effects of anesthetics on other types of cancer (e.g., breast cancer) requires further investigation.

In summary, these results suggested that the volatile anesthetic sevoflurane had protumor effects on tumor growth and metastasis of ovarian cancer, and intravenous anesthetic propofol had no significant effects, while local anesthetic lidocaine had antitumor effects on ovarian cancer. Overexpression of TASK-3 channels in ovarian cancer, especially in mitochondria, contributes to the differential effects of anesthetics on tumor growth and metastasis of ovarian cancer. These findings provide novel insights into the roles and underlying mechanism of TASK-3 channels in the effects of anesthetics on ovarian cancer biology and advance our knowledge of perioperative anesthetic management on postoperative cancer outcome.

Data availability statement

The data that support the findings of this study are available from the corresponding author (Xiangdong Chen) upon reasonable request.

Funding

This work was supported by grant 81571075 (to Xiangdong Chen) from the National Natural Science Foundation of China (Beijing, China).

Ethics approval and consent to participate

All animal experimental protocols were approved by the Animal Care and Use Committee of Huazhong University of Science and Technology (Wuhan, Hubei, China). Ethics approval for the study was granted by the local research ethics committee (Approval number:Y20170514). Specimens were collected with legal regulations, and informed consent was obtained from each patient.

CRediT authorship contribution statement

Zhiqiang Hu: Writing – review & editing, Writing – original draft, Investigation, Data curation, Conceptualization. **Qi Jia:** Writing – original draft, Investigation, Formal analysis, Data curation. **Shanglong Yao:** Writing – review & editing, Supervision, Resources. **Xiangdong Chen:** Writing – review & editing, Supervision, Resources, Funding acquisition, Conceptualization.

Declaration of competing interest

The authors declare that they have no known competing financial interests or personal relationships that could have appeared to influence the work reported in this paper.

Acknowledgments

The authors would like to acknowledge Hui Gao (Department of Obstetrics and Gynecology, Union Hospital, Tongji Medical College, Huazhong University of Science and Technology) for generously providing human ovarian specimens.

Appendix A. Supplementary data

Supplementary data to this article can be found online at https://doi.org/10.1016/j.heliyon.2024.e34973.

References

[1] S. Lheureux, et al., Epithelial ovarian cancer, Lancet 393 (2019) 1240–1253.
[2] E. Pujade-Lauraine, New treatments in ovarian cancer, Ann. Oncol. 28 (2017) viii57-viii60.
[3] T.J. Wigmore, et al., Long-term survival for patients undergoing volatile versus IV anesthesia for cancer surgery: a retrospective analysis, Anesthesiology 124 (2016) 69–79.
[4] D.I. Sessler, et al., Recurrence of breast cancer after regional or general anaesthesia: a randomised controlled trial, Lancet 394 (2019) 1807–1815.
[5] K.M. Elias, et al., Anesthetic selection and disease-free survival following optimal primary cytoreductive surgery for stage III epithelial ovarian cancer, Ann. Surg Oncol. 22 (2015) 1341–1348.
[6] T. Loop, et al., Sevoflurane inhibits phorbol-myristate-acetate-induced activator protein-1 activation in human T lymphocytes in vitro: potential role of the p38-stress kinase pathway, Anesthesiology 101 (2004) 710–721.
[7] A. Buckley, et al., Effect of anaesthetic technique on the natural killer cell anti-tumour activity of serum from women undergoing breast cancer surgery: a pilot study, Br. J. Anaesth. 113 (Suppl 1) (2014) i56–i62.
[8] M.W. Sekandarzad, et al., Perioperative anesthesia Care and tumor progression, Anesth. Analg. 124 (2017) 1697–1708.
[9] L.L. Benzonana, et al., Isoflurane, a commonly used volatile anesthetic, enhances renal cancer growth and malignant potential via the hypoxia-inducible factor cellular signaling pathway in vitro, Anesthesiology 119 (2013) 593–605.
[10] Q.Y. Shi, et al., Sevoflurane promotes the expansion of glioma stem cells through activation of hypoxia-inducible factors in vitro, Br. J. Anaesth. 114 (2015) 825–830.
[11] Z.F. Wu, et al., Propofol-based total intravenous anesthesia is associated with better survival than desflurane anesthesia in colon cancer surgery, Anesthesiology 129 (2018) 932–941.
[12] W. Xing, et al., Lidocaine induces apoptosis and suppresses tumor growth in human hepatocellular carcinoma cells in vitro and in a xenograft model in vivo, Anesthesiology 126 (2017) 868–881.
[13] M.Z. Johnson, et al., Effect of perioperative lidocaine on metastasis after sevoflurane or ketamine-xylazine anaesthesia for breast tumour resection in a murine model, Br. J. Anaesth. 121 (2018) 76–85.
[14] J. Freeman, et al., Effect of perioperative lidocaine, propofol and steroids on pulmonary metastasis in a murine model of breast cancer surgery, Cancers 11 (2019).
[15] A.B. Rajendra, et al., Effect of peritumoral infiltration of local anesthetic before surgery on survival in early breast cancer, J. Clin. Oncol. 41 (2023) 3318–3328.
[16] G. D'Agostino, et al., Lidocaine inhibits cytoskeletal remodelling and human breast cancer cell migration, Br. J. Anaesth. 121 (2018) 962–968.
[17] A.M. Zoey, et al., Lidocaine induces apoptosis in head and neck squamous cell carcinoma through activation of bitter taste receptor T2R14, Cell Rep. 42 (2023) 113437.
[18] Y. Kim, et al., TASK-3, a new member of the tandem pore K(+) channel family, J. Biol. Chem. 275 (2000) 9340–9347.
[19] R.M. Lazarenko, et al., Motoneuronal TASK channels contribute to immobilizing effects of inhalational general anesthetics, J. Neurosci. 30 (2010) 7691–7704.
[20] N.A. Guagliardo, et al., Adrenal tissue-specific deletion of TASK channels causes aldosterone-driven angiotensin II-independent hypertension, Hypertension 73 (2019) 407–414.
[21] A.M. Linden, et al., TASK-3 knockout mice exhibit exaggerated nocturnal activity, impairments in cognitive functions, and reduced sensitivity to inhalation anesthetics, J. Pharmacol. Exp. Therapeut. 323 (2007) 924–934.
[22] C. Yao, et al., TASK channels contribute to neuroprotective action of inhalational anesthetics, Sci. Rep. 7 (2017) 44203.
[23] G. Du, et al., TASK channel deletion reduces sensitivity to local anesthetic-induced seizures, Anesthesiology 115 (2011) 1003–1011.
[24] D. Mu, et al., Genomic amplification and oncogenic properties of the KCNK9 potassium channel gene, Cancer Cell 3 (2003) 297–302.
[25] L. Pei, et al., Oncogenic potential of TASK3 (Kcnk9) depends on K+ channel function, Proc. Natl. Acad. Sci. U.S.A. 100 (2003) 7803–7807.
[26] C.J. Kim, et al., Altered expression of KCNK9 in colorectal cancers, Apmis 112 (2004) 588–594.
[27] L. Kosztka, et al., Inhibition of TASK-3 (KCNK9) channel biosynthesis changes cell morphology and decreases both DNA content and mitochondrial function of melanoma cells maintained in cell culture, Melanoma Res. 21 (2011) 308–322.
[28] H. Sun, et al., A monoclonal antibody against KCNK9 K(+) channel extracellular domain inhibits tumour growth and metastasis, Nat. Commun. 7 (2016) 10339.
[29] K. Pocsai, et al., Melanoma cells exhibit strong intracellular TASK-3-specific immunopositivity in both tissue sections and cell culture, Cell. Mol. Life Sci. 63 (2006) 2364–2376.
[30] D. Nagy, et al., Silencing the KCNK9 potassium channel (TASK-3) gene disturbs mitochondrial function, causes mitochondrial depolarization, and induces apoptosis of human melanoma cells, Arch. Dermatol. Res. 306 (2014) 885–902.
[31] L. Marklund, et al., Cisplatin-induced apoptosis of mesothelioma cells is affected by potassium ion flux modulator amphotericin B and bumetanide, Int. J. Cancer 93 (2001) 577–583.
[32] L. Lin, et al., Anaesthetic technique may affect prognosis for ovarian serous adenocarcinoma: a retrospective analysis, Br. J. Anaesth. 106 (2011) 814–822.
[33] T. Piegeler, et al., Clinically relevant concentrations of lidocaine and ropivacaine inhibit TNFα-induced invasion of lung adenocarcinoma cells in vitro by blocking the activation of Akt and focal adhesion kinase, Br. J. Anaesth. 115 (2015) 784–791.
[34] L. Zhang, et al., Lidocaine inhibits the proliferation of lung cancer by regulating the expression of GOLT1A, Cell Prolif. 50 (2017) e12364.
[35] Y. Chen, et al., Lidocaine inhibited tendon cell proliferation and extracellular matrix production by down regulation of cyclin A, CDK2, type I and type III collagen expression, Int. J. Mol. Sci. 23 (2022) 8787.
[36] R. Zúñiga, et al., TASK-3 downregulation triggers cellular senescence and growth inhibition in breast cancer cell lines, Int. J. Mol. Sci. 19 (2018) 1033.
[37] X. Luo, et al., Impact of isoflurane on malignant capability of ovarian cancer in vitro, Br. J. Anaesth. 114 (2015) 831–839.
[38] M. Zhu, et al., Isoflurane enhances the malignant potential of glioblastoma stem cells by promoting their viability, mobility in vitro and migratory capacity in vivo, Br. J. Anaesth. 116 (2016) 870–877.
[39] R. Li, et al., Distinct effects of general anesthetics on lung metastasis mediated by IL-6/JAK/STAT3 pathway in mouse models, Nat. Commun. 11 (2020) 642.
[40] S. Ciechanowicz, et al., Differential effects of sevoflurane on the metastatic potential and chemosensitivity of non-small-cell lung adenocarcinoma and renal cell carcinoma in vitro, Br. J. Anaesth. 120 (2018) 368–375.
[41] K. Leithner, et al., TASK-1 regulates apoptosis and proliferation in a subset of non-small cell lung cancers, PLoS One 11 (2016) e0157453.

[42] S. Rinné, et al., The molecular basis for an allosteric inhibition of K^+-flux gating in K2P channels, Elife 8 (2019) e39476.
[43] K. Conway, et al., Covalent modification of a volatile anesthetic regulatory site activates TASK-3 (KCNK9) tandem-pore potassium channels, Mol. Pharmacol. 81 (2012) 393–400.
[44] C. Hu, et al., Sevoflurane but not propofol enhances ovarian cancer cell biology through regulating cellular metabolic and signaling mechanisms, Cell Biol. Toxicol. 39 (2023) 1395–1411.
[45] N. Kadiri, et al., Neurotensin inhibits background K+ channels and facilitates glutamatergic transmission in rat spinal cord dorsal horn, Eur. J. Neurosci. 34 (2011) 1230–1240.
[46] S. Bonnet, et al., A mitochondria-K+ channel axis is suppressed in cancer and its normalization promotes apoptosis and inhibits cancer growth, Cancer Cell 11 (2007) 37–51.
[47] B.G. Heerdt, et al., The intrinsic mitochondrial membrane potential of colonic carcinoma cells is linked to the probability of tumor progression, Cancer Res. 65 (2005) 9861–9867.
[48] Y.P. Ow, et al., Cytochrome c: functions beyond respiration, Nat. Rev. Mol. Cell Biol. 9 (2008) 532–542.
[49] S.H. Jang, et al., Nuclear localization and functional characteristics of voltage-gated potassium channel Kv1.3, J. Biol. Chem. 290 (2015) 12547–12557.
[50] B. Schlereth, et al., Eradication of tumors from a human colon cancer cell line and from ovarian cancer metastases in immunodeficient mice by a single-chain Ep-CAM-/CD3-bispecific antibody construct, Cancer Res. 65 (2005) 2882–2889.
[51] J.F. Liu, et al., Establishment of patient-derived tumor xenograft models of epithelial ovarian cancer for preclinical evaluation of novel therapeutics, Clin. Cancer Res. 23 (2017) 1263–1273.